

Osteoarthritis and Cartilage



Osteoarthritis-associated basic calcium phosphate crystals alter immune cell metabolism and promote M1 macrophage polarization

O.R. Mahon †‡, D.J. Kelly ‡§, G.M. McCarthy ||, A. Dunne †§¶*

† School of Biochemistry and Immunology, Trinity College Dublin, Dublin, Ireland

‡ Trinity Centre for Bioengineering, Trinity Biomedical Sciences Institute, Trinity College Dublin, Dublin, Ireland

§ Advanced Materials and Bioengineering Research (AMBER) Centre, Trinity College Dublin, Ireland

|| School of Medicine and Medical Science, University College Dublin and Misericordiae University Hospital, Dublin, Ireland Eccles Street, Dublin 1, Ireland

¶ School of Medicine, Trinity College Dublin, Dublin, Ireland

ARTICLE INFO

Article history:

Received 27 May 2019

Accepted 16 October 2019

Keywords:

Immunometabolism

Macrophage polarization

BCP crystals

Metabolic reprogramming

SUMMARY

Objective: A number of studies have demonstrated that molecules called 'alarmins' or danger-associated molecular patterns (DAMPs), contribute to inflammatory processes in the OA joint. Metabolic reprogramming of immune cells, including macrophages, is emerging as a prominent player in determining immune cell phenotype and function. The aim of this study was to investigate if basic calcium phosphate (BCP) crystals which are OA-associated DAMPs, impact on macrophage phenotype and metabolism.

Methods: Human monocyte derived macrophages were treated with BCP crystals and expression of M1 (CXCL9, CXCL10) and M2 (MRC1, CCL13)-associated markers was assessed by real-time PCR while surface maturation marker (CD40, CD80 & CD86) expression was assessed by flow cytometry. BCP induced metabolic changes were assessed by Seahorse analysis and glycolytic marker expression (hexokinase 2(HK2), Glut1 and HIF1 α) was examined using real-time PCR and immunoblotting.

Results: Treatment with BCP crystals upregulated mRNA levels of CXCL9 and CXCL10 while concomitantly downregulating expression of CCL13 and MRC1. Furthermore, BCP-treated macrophages enhanced surface expression of the maturation makers, CD40, CD80 and CD86. BCP-treated cells also exhibited a shift towards glycolysis as evidenced by an increased ECAR/OCR ratio and enhanced expression of the glycolytic markers, HK2, Glut1 and HIF1 α . Finally, BCP-induced macrophage activation and alarmin expression was reduced in the presence of the glycolytic inhibitor, 2-DG.

Conclusions: This study not only provides further insight into how OA-associated DAMPs impact on immune cell function, but also highlights metabolic reprogramming as a potential therapeutic target for calcium crystal-related arthropathies.

© 2019 Osteoarthritis Research Society International. Published by Elsevier Ltd. All rights reserved.

Introduction

Osteoarthritis (OA) is the most common form of chronic arthropathy and leading cause of disability worldwide. It affects 10% of males and 18% of females over the age of 45, a figure that is set to rise as life expectancy increases^{1,2}. In addition, the current obesity epidemic has resulted in an increased incidence of OA in younger individuals, many of whom will undergo multiple joint replacements due to the limited lifespan of artificial joints.

Extensive research has highlighted a complex interplay between chondrocytes, synovial fibroblasts and the innate immune network and while much progress has been made in elucidating the cellular and molecular events contributing to OA, the complex nature of the disease has hampered the development of a successful disease-modifying drug. Current therapies are focused on providing symptomatic relief rather than halting or reversing disease progression, hence, there is a clear need to identify specific orchestrators that initiate and/or contribute to eventual joint destruction.

Immunometabolism is an emerging field of research that focuses on changes in intracellular metabolic pathways in immune cells and how these alterations impact on cell fate and function^{3–5}. It is now recognised that a metabolic shift from oxidative phosphorylation to a highly metabolically active glycolytic state

* Address correspondence and reprint requests to: School of Biochemistry & Immunology and School of Medicine, Trinity Biomedical Sciences Institute, Trinity College Dublin, Ireland. Tel: 353-1 8962437.

E-mail address: aidunne@tcd.ie (A. Dunne).

(designed to maintain energy homeostasis under conditions of low oxygen and acute stress) can lead to an accumulation of reactive oxygen species (ROS) and metabolic intermediates that promote the synthesis of degradative enzymes and inflammatory mediators⁶. Increased glycolytic rates and glucose consumption are associated with enhanced expression of the glucose transporter, GLUT1, as well as elevated lactate production⁷. Furthermore, activated immune cells exhibit Warburg metabolism and HIF-1 α induction even under normoxic conditions^{8,9}. Recent studies have also demonstrated that macrophage activation and phenotype is intricately linked to cellular metabolic status. For example, lipopolysaccharide (LPS) activated M1 macrophages [M1(LPS)] exhibit an enhanced glycolytic profile characterised by increased expression of glucose transporters, glycolytic enzymes and rapid production of ATP^{3,10,11}. While this metabolic switch is required to meet the energy demands of the cell during infection and provide biosynthetic components required to carry out effector functions, dysregulated immune-cell metabolism which results in sustained inflammatory responses, has been linked to a number of debilitating diseases and it has been strongly suggested that strategies to modulate metabolic reprogramming represents a novel approach to regulate disease pathology^{12–15}. Furthermore, a number of metabolites have been shown to alter macrophage polarization and there is now a host of studies demonstrating how inhibitors of metabolism (e.g., glycolysis, fatty acid synthesis and fatty acid oxidation) can regulate immune responses providing potential new avenues to manipulate immune cell activation¹⁵.

Altered immunometabolism has been recognised as a component of a number of inflammatory and autoimmune conditions^{13–17} and while it is well established that glycolysis is important for energy production in chondrocytes, there is now also evidence for increased glycolysis and deregulated cellular metabolism in OA^{18–21}. Indeed, mitochondrial dysfunction is a hallmark of OA and previous studies have shown increased mitochondrial DNA damage in OA chondrocytes compared to healthy controls suggesting that cartilage degradation during OA and normal cartilage aging may be metabolically different processes²². Furthermore, lactate levels are elevated in OA and are frequently co-associated with crystal arthropathy comorbidities^{23,24}. Indeed, one notable link between mechanical and inflammatory mechanisms in OA pathogenesis is calcium crystal deposition. Basic calcium phosphate (BCP) crystals, comprised mainly of hydroxyapatite, are uniquely associated with OA and have been identified in 100% of cartilage and 50% of synovial fluid samples at the time of joint replacement where their concentration correlates with the severity of histological and radiographic OA²⁵. Crystal deposition and articular calcification occurs as a result of dysregulated ossification processes and an imbalance between pro-mineralization and anti-mineralization factors. Direct injection of BCP-crystals into mouse knees results in synovial inflammation, cartilage destruction and chondrocyte apoptosis²⁶. As a result, these crystals are now considered damage-associated molecular patterns (DAMPs) or 'alarmins' as they can activate fibroblasts, macrophages and chondrocytes through a variety of signaling pathways which, in turn, leads to the production of inflammatory and catabolic mediators^{27–32}. While several pathological cellular mechanisms have been identified, studies examining the effects of BCP crystals in humans are lacking as are drugs that prevent crystal deposition, permit crystal dissolution or specifically target the pathogenic effects that result in clinical manifestations. In this study we demonstrate that BCP crystals polarize primary human macrophages towards an M1-like phenotype and upregulate the expression of glycolytic markers. This is accompanied by a bioenergetics switch in favour of glycolysis. Furthermore, we demonstrate that targeting glycolysis reduces BCP-induced macrophage polarization and alarmin

expression, suggesting that calcium crystal deposition impacts on immune cell metabolic reprogramming and subsequent macrophage phenotype and function.

Methods

Reagents and assessment of endotoxin contamination in BCP preparations are described in supplementary methods.

Human blood monocyte-derived macrophage isolation

This study was approved by the research ethics committee of the School of Biochemistry and Immunology, Trinity College Dublin and was conducted in accordance with the Declaration of Helsinki. Leucocyte-enriched buffy coats from anonymous healthy donors were obtained with permission from the Irish Blood Transfusion Board (IBTS), St. James's Hospital, Dublin. Donors provided informed written consent to the IBTS for their blood to be used for research purposes. PBMC were isolated and differentiated into macrophages as described previously³³. The purity of CD14⁺CD11b⁺ macrophages was assessed by flow cytometry and was routinely >95% (Fig. S1).

Cytokine measurements

Cells were pre-treated with PD98059 (20 μ M), SB203580 (20 μ M), for 45 min prior to stimulation with BCP crystals (50 μ g/ml) for 24 h. Supernatants were harvested and cytokine concentrations of TNF α , IL-6 and IL-8 were quantified by ELISA (eBioscience, San Diego, CA) according to manufacturer's protocol.

Real-time PCR

Macrophages were treated with BCP crystals (50 μ g/ml) alone or in the presence of indicated inhibitors (PD98059 (20 μ M), SB203580 (20 μ M), Latrunculin B (1 μ M), Cytochalasin D (5 μ M), Cytochalasin B (5 μ M), Dynasore (80 μ M) or 2-DG (25 mM). RNA was extracted using High-Pure RNA Isolation Kits (Roche), and assessed for concentration and purity using the NanoDrop 2000c UV-Vis spectrophotometer. RNA was equalised and reverse transcribed using the Applied Biosystems High-Capacity cDNA reverse transcription kit. Real-time PCR carried out on triplicate cDNA samples using the CFX96 Touch Real-Time PCR Detection System (Bio-Rad Laboratories, California). Reactions included iTaq Universal SYBR Green Supermix (Bio-rad Laboratories), cDNA, TaqMan fast universal PCR Master Mix and pre-designed TaqMan gene expression probes (Applied Biosystems) for CXCL9, CXCL10, MRC1, CCL13, S100A8 and the housekeeping gene, 18S ribosomal RNA. The $2^{-\Delta\Delta CT}$ method was used to analyse relative gene expression. Oligonucleotide primer sequences for SYBR primers for HK2, Glut1, HIF1 α , HIF2, GAPDH and HRPTL are provided in [Supplementary Table 1](#).

Immunoblotting

Primary macrophages were stimulated BCP crystals (50 μ g/ml) for 3, 6, or 24 h for the detection Hexokinase 2 (HK2), Glut1 or HIF1 α protein. Cells were lysed by addition of RIPA buffer (Tris 50 mM; NaCl 150 mM; SDS 0.1%; sodium deoxycholate 0.5%; Triton X 100). Lysates were electrophoresed on SDS-PAGE gels (12% gel for Glut1, 10% gel for HK2 and 7.5% gel for HIF1 α) and transferred to PVDF membranes (Millipore, Massachusetts) prior to detection with anti-HK2 or anti-Glut1 antibodies ([Supplementary Table 2](#)).

Flow cytometry

Primary human macrophages were plated at a concentration of 1×10^6 cells/ml and stimulated with BCP crystals (50 $\mu\text{g/ml}$) for 24 h in the absence or presence of the glycolytic inhibitor 2-DG (25mM). Cells were collected, washed, Fcy blocked and stained extracellularly with amine-binding markers for dead cells (Fixable Viability Dye; eBioscience) for 10 min. Cells were washed in PBS and stained with fluorochrome-conjugated antibodies specific for CD14, CD11b, CD86, CD40 and CD80 (all eBiosciences) and fixed with 2% paraformaldehyde (PFA) washed and acquired. The model antigen DQ-Ova, which fluoresces upon processing by proteases inside the cell, was used to assess phagocytic capacity of the cells. Macrophages were cultured with complete RPMI containing DQ-Ovalbumin (500 ng/ml; Invitrogen) for 20 min at 37 °C, followed by incubation for 10 min at 4 °C. Cells were then washed in PBS and immediately acquired. Cells were acquired on a FACSCanto TM II (BD Biosciences) and analysis was performed with FlowJo v.10 software (Tree Star Inc.). Gating strategies utilised in all experiments are detailed in [Supplementary Fig. 1](#).

Seahorse analyser

Macrophages were cultured at 1×10^6 cells/ml for 6 days prior to re-seeding at 2×10^5 cells/well in a Seahorse 96-well microplate and allowed to rest for 5 h prior to BCP or LPS stimulation. The Seahorse cartridge plate was hydrated with XF calibrant fluid and incubated in a non-CO₂ incubator at 37°C for a minimum of 8 h prior to use. To determine the effect of BCP crystals, macrophages were incubated with BCP crystals (50 $\mu\text{g/ml}$) for 24 h, prior to analysis using a Seahorse XFe24 analyser. 30 min prior to placement into the XF/XFe analyser, cell culture medium was replaced with complete XF assay medium (Seahorse Biosciences; supplemented with 10mM glucose, 1mM sodium pyruvate, 2mM L-glutamine, and pH adjusted to 7.4) and incubated in a non-CO₂ incubator at 37°C. Blank wells (XF assay medium only) were prepared without cells for subtracting the background oxygen consumption rate (OCR) and extracellular acidification rate (ECAR) during analysis. Oligomycin (1 μM ; Cayman Chemicals), carbonyl cyanide-p-trifluoromethoxyphenylhydrazone (FCCP) (1 μM ; Santa Cruz biotechnology), rotenone (500 nM), and antimycin A (500 nM) and 2-deoxy-D-glucose (2-DG) (25 mM; all Sigma-Aldrich) were prepared in XF assay medium and loaded into the appropriate injection ports on the cartridge plate and incubated for 10 min in a non-CO₂ incubator at 37°C. OCR and ECAR were measured over time with sequential injections of oligomycin, FCCP, rotenone and antimycin A and 2-DG. Analysis of results was performed using Wave software (Agilent Technologies). The rates of basal glycolysis, max glycolysis, glycolytic reserve etc. were calculated as detailed in the manufacturer's protocol and supplied in [Supplementary Table 3](#).

Statistical analysis

Each experiment was performed in at least four healthy donors (defined by N) with 3–4 technical replicates run for each experiment, (defined by n) depending on the assay type. Paired one-way ANOVA or Kruskal–Wallis tests were used for the comparison of more than two groups for parametric and non-parametric analysis respectively, with the Tukey or Dunn's post-test (where applicable). A paired Student's *t*-test was used when there were only two groups for analysis and the data was normally distributed and a Two-tailed paired Wilcoxon Signed rank test was used for non-parametric data. All statistical analysis was performed on

GraphPad Prism 7.00 (GraphPad Software). *P* value < 0.05 were deemed significant.

Results

BCP crystals promote M1 macrophage polarization

We and others have previously reported that BCP-crystals drive inflammatory mediator and alarmin production in macrophages, fibroblasts and chondrocytes^{27,29,32}. In order to determine if BCP crystals impact on macrophage polarization, primary human macrophages were treated with previously published doses of BCP crystals (50 $\mu\text{g/ml}$) for 24 h and expression of established genes associated with M(LPS) (i.e., prototypic M1-like MDMs) and M(IL-4) (i.e., prototypic M2-like MDMs) macrophage polarization was assessed by real-time PCR. While BCP stimulation of macrophages significantly enhanced the mRNA expression of the M(LPS) markers, CXCL9 and CXCL10, compared to control samples, treatment of macrophages with the crystals led to a significant decrease in basal levels of the M(IL-4) macrophage markers, MRC1 and CCL13 [Fig. 1(A)–(D)]. Furthermore, treatment of macrophages with BCP crystals significantly enhanced secretion of the chemokine, IL-8 [Fig. 1 (E)]. Treatment of macrophages with BCP-crystals did not induce secretion of the cytokines TNF α or IL-6 (Fig. S2(A)) which is in agreement with published results examining BCP-induced responses in macrophages³⁰ and together with results from the HEK-Blue™ hTLR4 assay system (Invivogen) (Fig. S2(B)) signifies a lack of endotoxin contamination in our BCP crystal preparation.

We have previously demonstrated that BCP crystals activate MAPKs downstream of Syk in a receptor independent manner^{29,30}. Pre-treatment of macrophages with either SB203580 or PD98059 to inhibit p38 and ERK, respectively, significantly inhibited BCP-induced IL-8, CXCL9 and CXCL10 expression [Fig. 1(F)–(H)], demonstrating that MAPK activation is also involved BCP-induced macrophage polarization. Of note, inhibition of MAPKs had no effect on MRC1 or CCL13 mRNA expression in BCP treated macrophages (Fig. S3). In addition to CXCL9/10 expression, we assessed surface expression of the M1-associated maturation markers, CD86, CD80, CD40 [Fig. 1(I) and (J)]. BCP crystals stimulation induced a significant increase in the expression of CD86 and CD40, and although not significant, a trend towards increased CD80 surface marker expression was also observed ($p = 0.0674$). Finally, the phagocytic capacity of macrophages was assessed following BCP stimulation given that activated M1-like macrophages reduce their phagocytic capacity upon activation³⁴. Cells were incubated with FITC-conjugated DQ-Ovalbumin (DQ-Ova) at 500 ng/ml post BCP stimulation and analysed for antigen uptake by flow cytometry. As expected, unstimulated macrophages exhibited high DQ-Ova uptake, however, this was significantly reduced upon stimulation of cells with BCP crystals [Fig. 1(K) and (L)].

BCP crystals alter macrophage metabolism and promote glycolysis

A number of studies have demonstrated that activated macrophages exhibit an enhanced glycolytic profile characterised by increased expression of glucose transporters and glycolytic enzymes³⁵. In order to determine whether BCP crystal-induced macrophage polarization coincided with a metabolic switch favoring glycolysis, macrophages were treated with BCP and established markers of glycolysis were assessed by real-time PCR and immunoblotting. BCP crystals significantly upregulated mRNA expression of the glucose transporter, GLUT 1 the glycolytic enzyme, hexokinase 2 (HK2) and the transcription factor, HIF1 α . There was also a trend towards increased expression of

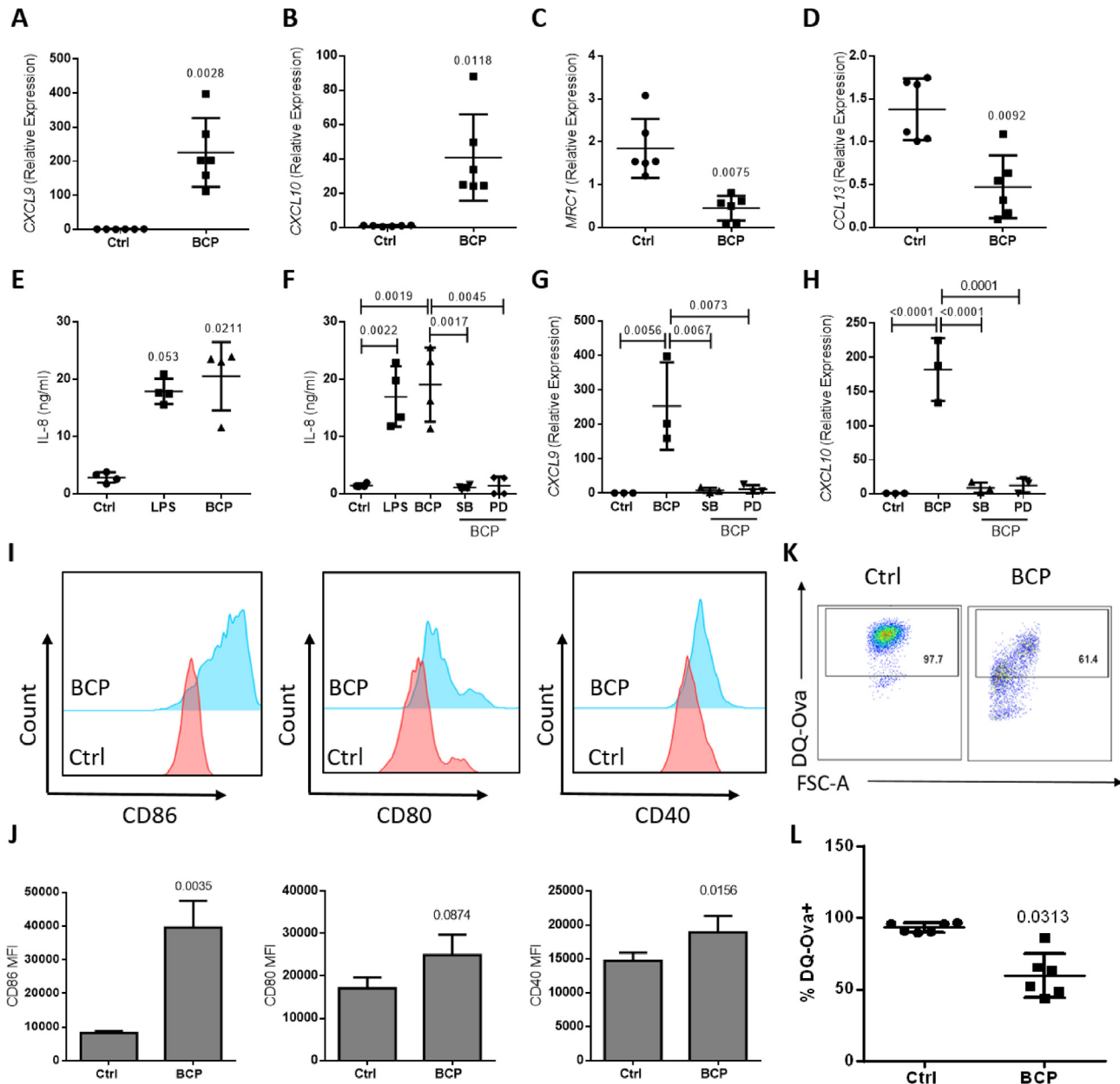


Fig. 1. BCP crystals promote M1 macrophage polarization. Primary human macrophages (1×10^6) were stimulated with BCP (50 $\mu\text{g/ml}$) for 24 h. (A–D) mRNA expression of CXCL9, CXCL10, MRC1 and CCL13 was analysed by real-time PCR ($N = 6$, $n = 3$). (E) IL-8 cytokine production in cell supernatants was analysed by ELISA ($N = 4$, $n = 3$). (F–H) Macrophages were pre-treated with the p38 and ERK MAP kinase inhibitors (SB203580; 20 μM , PD98059; 20 μM) for 45 min prior to stimulation with BCP (50 $\mu\text{g/ml}$) for 24 h. IL-8 cytokine production in cell supernatants was analysed by ELISA ($N = 4$, $n = 3$) and mRNA levels of CXCL9 and CXCL10 were analysed by real-time PCR ($N = 6$, $n = 3$). (I) Representative histograms from one experiment of the macrophage maturation markers CD86, CD80 and CD40 were determined by flow cytometry and (J) Pooled data ($N = 5$, $n = 2$) depicts mean Fluorescence Intensity (MFI) of surface marker expression. Macrophages were stimulated with BCP (50 $\mu\text{g/ml}$) for 24 h and then incubated with FITC-conjugated DQ-ovalbumin (DQ-Ova; 500 ng/ml) for 20 min prior to analysis by flow cytometry. (K) Representative dot plots depicting DQ-Ova uptake by BCP treated macrophages. (L) Pooled data ($N = 5$, $n = 2$) depicts percentage DQ-Ova uptake. All data is represented as Mean \pm SEM. Data was analysed using Kruskal Wallis with Dunn's post-test for cytokine assays and one-way ANOVA with Tukey post-test for real-time PCR assays. Data was analysed using Wilcoxon Signed Rank test for Flow Cytometry assays.

glyceraldehyde-3-phosphate dehydrogenase (GAPDH) ($p = 0.0634$) [Fig. 2(A)]. No difference in mRNA expression of HIF2 α was observed (Fig. S4). Furthermore, protein levels of both HK2 and GLUT1 and were found to be highly expressed at 24 h post BCP crystal treatment, while increased expression of HIF1 α was observed at 3, 6 and 24 h post stimulation [Fig. 2(B)]. Densitometric analysis revealed a dose dependent upregulation of HK2 and GLUT1 proteins at 3, 6 and 24 h with maximal and significant upregulation occurring at 24 h for both proteins [Fig. 2(C)]. To further investigate whether BCP treated cells were altering their energy metabolism to

a more glycolytic state, we measured both glycolysis and oxidative phosphorylation using the Seahorse XF-Analyzer. Macrophages were seeded into a Seahorse microplate and stimulated with BCP crystals for 3, 6 or 24 h. The rates of glycolysis and oxidative phosphorylation were determined by the measurement of ECAR (extracellular acidification rate) and OCR (oxygen consumption rate), respectively, before and after injections of oligomycin, FCCP, rotenone, antimycin A and 2-DG. Overall, the ECAR of BCP-treated cells was higher than untreated controls with the highest ECAR observed at 3 h post-stimulation [Fig. 2(D)]. The basal rate of

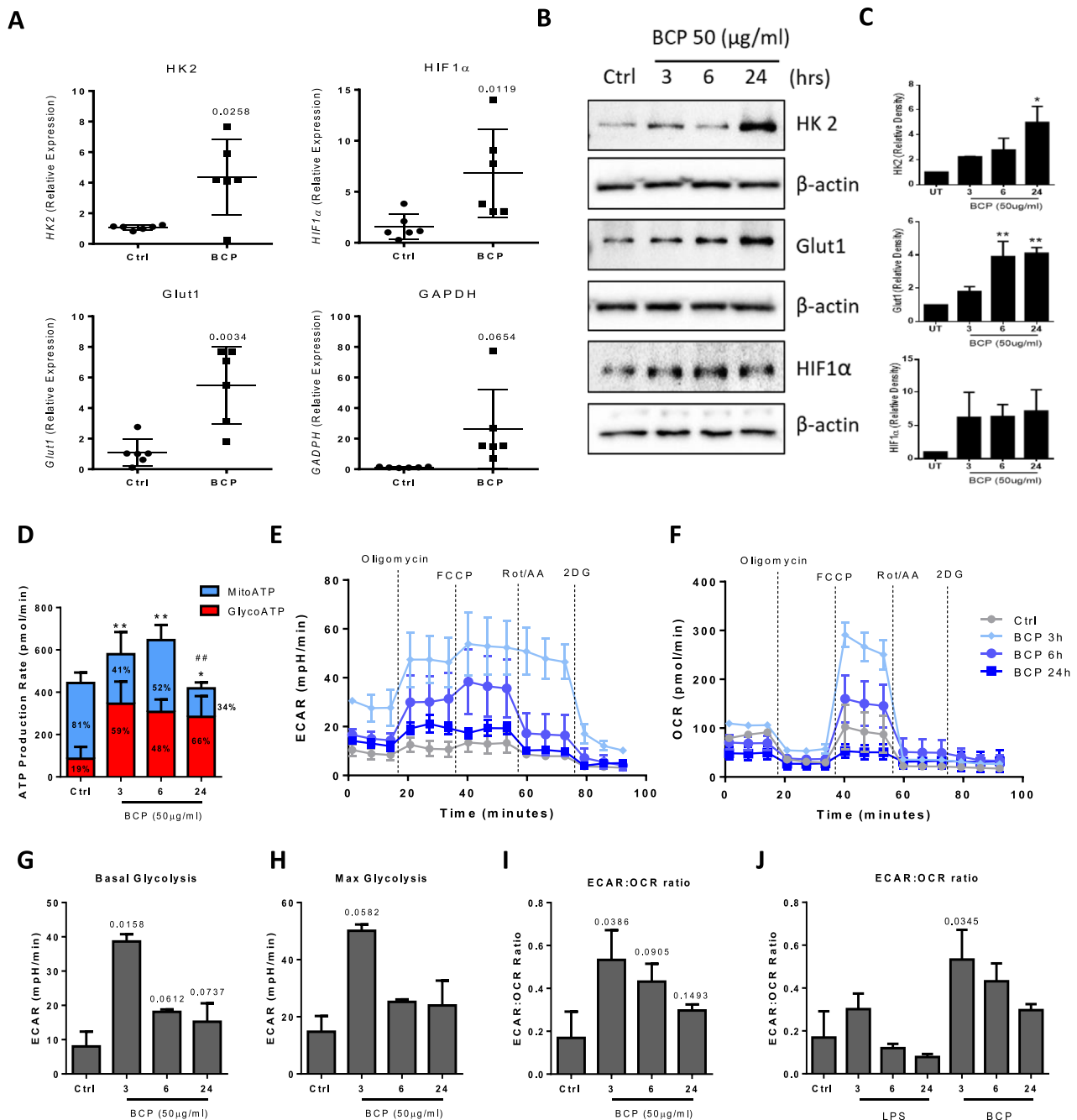


Fig. 2. BCP crystals alter macrophage metabolism and promote glycolysis. Primary human macrophages (1×10^6) were stimulated with BCP (50 μ g/ml) for 24 h. (A) mRNA expression of glycolytic markers GLUT1, HK2, HIF1 α and GAPDH were analysed by real-time PCR ($N = 6$, $n = 3$). (B) Representative western blots demonstrating expression of HK2 and Glut 1 in whole cell lysates in response to BCP crystals over time. (C) Densitometric analysis of immunoblots ($N = 3$) using ImageJ software. Bar graphs illustrate the Mean \pm SEM increase in protein expression relative to untreated control and normalised to β -actin housekeeping protein. (D & E) Representative glycolysis (ECAR) and oxidative phosphorylation (OCR) Seahorse bioenergetics profiles before and after injections of oligomycin (1 μ M), FCCP (1 μ M), antimycin A (500 nM)/Rotenone (500 nM), and 2-DG (25 mM) post stimulation with BCP crystals (50 μ g/ml). Bar graphs demonstrating (F) ATP production rate (G) basal glycolysis, (H) max glycolysis and (I) the ratio of glycolysis: oxidative phosphorylation (ECAR:OCR) in response to BCP crystal stimulation or (J) ECAR:OCR ratio in LPS or BCP treated cells. ($N = 3$, $n = 4$). All data is represented as Mean \pm SEM. Data was analysed using a paired Student's t test for real-time PCR assays, a one-way ANOVA for densitometric analysis of immunoblots. Data was analysed using Kruskal Wallis with Dunn's post-test was used for all Seahorse calculations.

glycolysis was increased in BCP-treated macrophages at all time points, compared to that of untreated control cells [Fig. 2(G)], while the maximum rate of glycolysis, was also enhanced in BCP stimulated cells, peaking at 3 h [Fig. 3(H)]. The respiratory profiles of macrophages appeared to mirror their observed glycolytic activity with 3 and 6 h BCP stimulation inducing the highest OCR, while 24 h stimulation appeared to marginally reduce OCR [Fig. 2 (E)].

This was reflected in the calculated basal respiration and max respiration (Fig. S5). Importantly, the ECAR:OCR ratio was increased in BCP treated cells at all time points tested [Fig. 2 (I)]. We also compared the metabolic profile of BCP-treated cells to that of a known PAMP, LPS which was marginally more potent than BCP at driving CXCL9 and CXCL10 gene expression (Figs. S6(I) and (J)). While both treatments enhanced glycolysis as well as oxidative

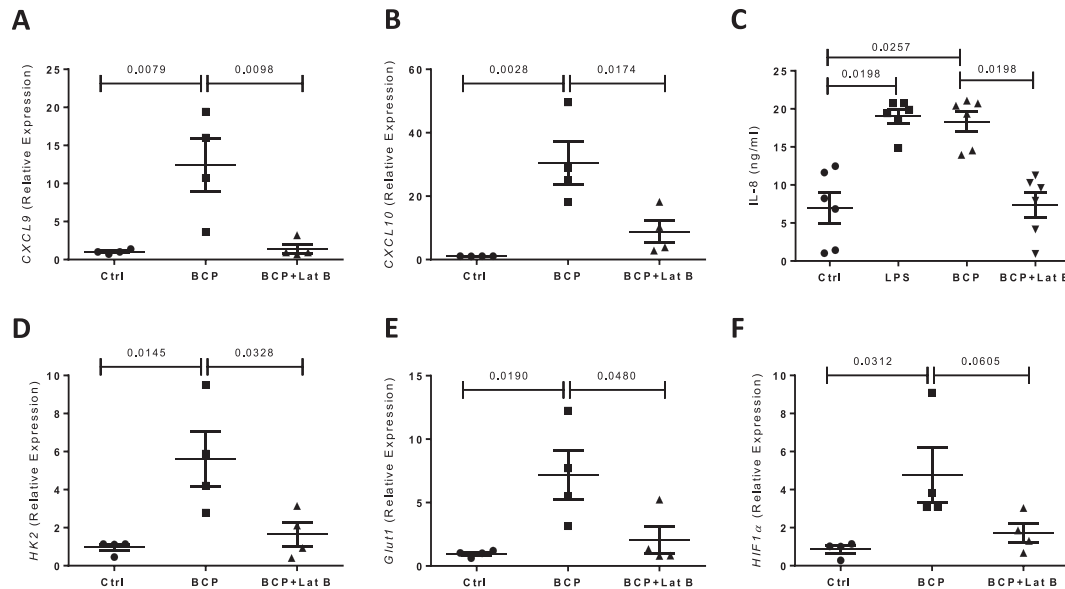


Fig. 3. Macrophage polarization and metabolic reprogramming by BCP crystals is dependent on particle uptake. Primary human macrophages (1×10^6) were treated with BCP (50 $\mu\text{g/ml}$) alone or were pre-treated with the actin polymerization inhibitor, Latrunculin B (1 μM), prior to treatment with BCP (50 $\mu\text{g/ml}$). (A & B) Graphs demonstrating mRNA levels of CXCL9 and CXCL10 ($N = 4$, $n = 3$). (C) Cytokine levels of IL-8 in cell supernatants ($N = 6$, $n = 3$). (D–F) mRNA expression of the glycolytic markers HK2, Glut1 and HIF1 α ($N = 4$, $n = 3$). Data is represented as Mean \pm SEM and analysed using Kruskal Wallis with Dunn's post-test for cytokine assays and one-way ANOVA with Tukey post-test for real-time PCR assays.

phosphorylation (Figs. S5(A)–(H)), overall the ECAR/OCR ratio was higher for BCP-treated macrophages suggesting that it may be a more potent inducer of glycolysis [Fig. 2(J)]. Furthermore, when ATP production rate was assessed post BCP treatment, total cellular ATP was significantly enhanced at all time points tested, with BCP-treatment resulting in an increase in glycoATP production rates and a decrease in mitoATP production rates [Fig. 2(D)]. Taken together, these data indicate that human macrophages promote glycolytic metabolism upon BCP stimulation.

Macrophage polarization and metabolic reprogramming by BCP crystals is dependent on particle uptake

Having established that BCP crystals can induce a metabolic switch in human macrophages, it was of interest to determine if these responses are dependent on particle uptake. To test this, macrophages were pre-treated with the actin polymerization inhibitor, Latrunculin B (1 μM) (to inhibit phagocytosis) for 45 min prior to stimulation with BCP crystals. Results demonstrate that BCP induced CXCL9 and CXCL10 mRNA expression was significantly reduced in the presence of latrunculin B [Fig. 3(A) and (B)]. Inhibition of particle uptake also significantly reduced BCP crystal induced IL-8 production [Fig. 3(C)] as well as mRNA expression of the glycolytic markers, HK2, Glut1 and HIF1 α [Fig. 3(D)–(F)]. To ensure that these observations were not due to loss of membrane integrity, which has been associated with Latrunculin B³⁶, cells were also pre-treated with the alternative actin polymerization inhibitors Cytochalasin D and B (5 μM) and the dynamin inhibitor, Dynasore (80 μM) prior to stimulation with BCP crystals. Similar trends were observed with all three inhibitors of phagocytosis (Fig. S7). Taken together, this indicates that particle uptake is essential for BCP crystal mediated activation of macrophages and glycolytic gene expression.

Inhibition of glycolysis abrogates BCP crystal induced macrophage polarization and alarmin expression

To elucidate if direct inhibition of glycolysis abrogates BCP crystal induced macrophage polarization, cells were stimulated with BCP crystals as described, in the presence or absence of the glycolytic inhibitor, 2-DG. Pre-treatment of cells with 2-DG resulted in a significant decrease of BCP induced CXCL9 and CXCL10 mRNA expression [Fig. 4(A) and (B)]. We have previously demonstrated that BCP crystals strongly upregulate expression of the alarmin S100A8^{29,30} which together with S100A9, is heavily implicated in driving catabolic processes in OA^{37–39}. mRNA expression of S100A8 was significantly inhibited in the presence of 2-DG [(Fig. 4(C)] suggesting that inhibition of macrophage metabolic reprogramming impacts on the ability of BCP crystals to induce alarmin expression. Finally, inhibition of glycolysis with 2-DG decreased surface marker expression of CD40, CD80 and CD86 in BCP treated macrophages [Fig. 4(D) and (E)]. Taken together, the results suggest that glycolytic blockade inhibits BCP-induced pro-inflammatory effects in macrophages.

Discussion

While several studies have demonstrated that impaired mitochondrial dysfunction contributes to pro-catabolic processes in OA chondrocytes, the factors contributing to this phenomenon have not been fully characterized²¹. Furthermore, there have been few studies examining metabolic reprogramming in OA synovial fibroblasts or macrophages. During infection, stimulation of pattern recognition receptors (PRRs) leads to enhanced glycolysis which enables immune cells to generate sufficient ATP and pro-inflammatory mediators required to carry out effector functions³. It is now well accepted that sterile tissue injury can provoke an immune response analogous to that seen during infection and that

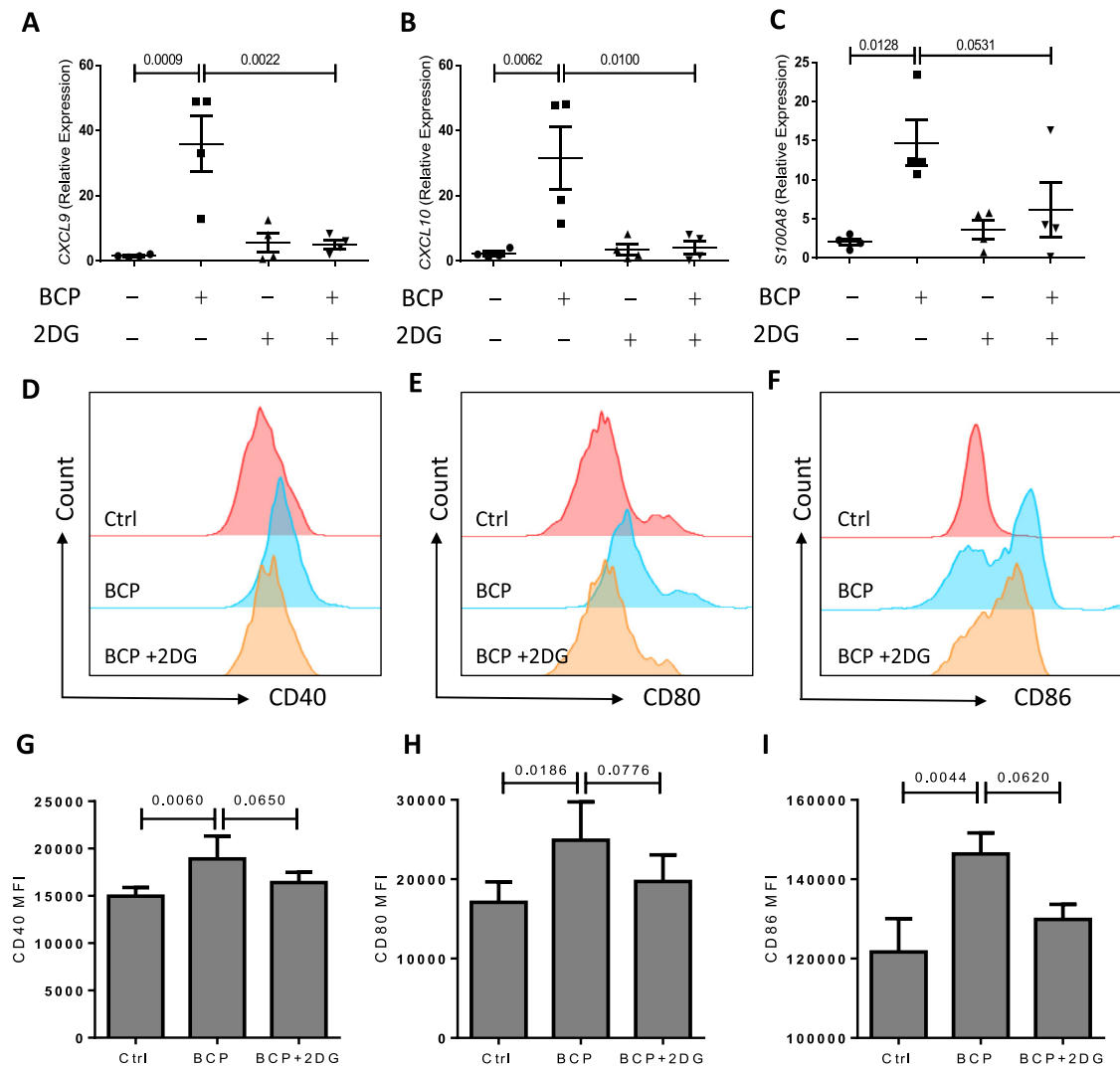


Fig. 4. BCP crystal-induced macrophage polarization is reduced in the presence of the glycolytic inhibitor 2-DG. Primary human macrophages (1×10^6) were stimulated with BCP (50 $\mu\text{g/ml}$) in the presence or absence of 2-DG (25mM) for 24 h. (A–C) Graphs demonstrating mRNA levels of CXCL9, CXCL10 and S100A8 ($N = 4$, $n = 3$). (D) Representative histograms from one experiment demonstrating CD40, CD80 and CD86 surface marker expression. (E) Pooled data ($N = 4$, $n = 2$) depicts mean Fluorescence Intensity (MFI) of surface marker expression. Data is represented as Mean \pm SEM Data and was analyzed using one-way ANOVA with Tukey post-test for real-time PCR assays and Kruskal Wallis for Flow cytometry assays.

endogenous molecules generated upon tissue damage are capable of exerting similar effects on cellular processes. Hence, while the switch to a highly active metabolic state is necessary for immune cell activation during infection, metabolic reprogramming by DAMPs/alarmins in the absence of infection has the potential to exacerbate existing inflammation. We now demonstrate that BCP crystals which are OA-associated DAMPs, polarize primary human macrophages towards an M1-like phenotype, enhancing expression of M1-macrophage associated markers and elevating expression of surface maturation markers. Furthermore, BCP crystal stimulation promotes a bioenergetic switch favouring glycolysis and this is accompanied by increased expression of HIF1 α , GLUT1 and hexokinase 2, all of which are surrogate markers of glycolysis. Finally, BCP-induced expression of M1 markers and the alarmin, S100A8, was inhibited in the presence of glycolytic inhibitor, 2DG, suggesting that BCP-induced macrophage polarization and inflammation may be dependent on metabolic reprogramming.

Particulates such as calcium oxalate crystals have previously been reported to promote M1 macrophage polarization⁴⁰ and, while a number of studies have investigated metabolic

reprogramming in human immune cells in response to exogenous pathogen associated molecules (i.e., PAMPs), to our knowledge this is the first report of an endogenous particulate impacting on immune cell metabolism. We demonstrate that human macrophages stimulated with BCP crystals upregulate both glycolysis and oxidative phosphorylation within hours of activation however, the overall glycolytic and ATP production rate is higher. In our hands, LPS stimulation also resulted in enhanced glycolysis and oxidative phosphorylation in human macrophages however, BCP crystals promoted a higher ECAR:OCR ratio than LPS which is considered a potent PAMP. The observed effects of LPS on ECAR and OCR rates differs from reports in murine DC demonstrating that LPS strongly upregulates aerobic glycolysis whilst simultaneously down-regulating oxidative phosphorylation via the action of iNOS-derived NO^{41,42}. There is, however, controversy regarding the expression/activity of iNOS in human immune cells^{43,44} and our finding is in agreement with a recent study by Malinarich *et al.* who reported that, while mature human DC are more glycolytic than immature DC, they do not entirely downregulate oxidative phosphorylation, and instead display a more “balanced” switch to

glycolysis whereby glycolysis and oxidative phosphorylation are both upregulated⁴⁵.

BCP crystals have previously been reported to upregulate the expression of inflammatory and catabolic mediators in a number of cell types implicated in OA^{24,46–48}. Our results show that, in addition to cytokines, chemokines and MMPs, BCP crystals can also upregulate expression of the key glycolytic enzymes, hexokinase 2, GLUT1 and HIF1 α , an effect which was attenuated in the presence of phagocytosis inhibitors. Furthermore, when glycolysis was inhibited with the glucose analog, 2-DG, we observed a notable decrease in M1-macrophage marker expression, in addition to S100A8, which is a key OA-associated DAMP. Further analysis will determine if metabolic targeting impacts on downstream targets of S100A8 which include cytokines such as IL-6 and IL-8, as well as MMPs 1, 9 and 13^{29,49}. Interestingly, BCP crystals themselves were potent drivers of IL-8 expression in our hands. This may represent a feed forward mechanism whereby BCP-induced S100A8 drives expression of IL-8, albeit it should be noted that, while S100A8 is known to stimulate the synovial membrane to generate pro-inflammatory mediators, including IL-8⁵⁰ in OA, this chemokine is generally not implicated in Milwaukee Shoulder Syndrome which is also characterized by BCP crystal deposition²⁵. Further study is required to fully elucidate the relationship between BCP crystals, IL-8 and the downstream effects of S100A8 production. It will also be necessary to determine whether BCP crystals drive metabolic reprogramming in synoviocytes from OA patient samples and whether glycolytic inhibitors impact on inflammatory/catabolic processes. Indeed, upregulation of glucose transport and an increase in glycolytic metabolism has been demonstrated in OA and particularly in chondrocytes where accumulation of lactic acid contributes to matrix acidification and impaired ECM synthetic function^{51–54}. Less is known regarding metabolic disturbances in OA-synoviocytes, however an increase in the glycolysis/OXPHOS ratio has been observed in OA-FLS²¹. Furthermore, silencing of PHD2, a global negative regulator of HIF-1 α expression decreased expression of angiogenic genes, while high glucose levels were shown to induce ROS and VEGF in OA-FLS further implicating a metabolic switch and increased glucose transport in synovial joint cells in OA^{55,56}.

While the field of immunometabolism is still in its infancy and much remains to be learned regarding the impact of metabolic reprogramming on disease pathogenesis, ultimately it may be possible to modulate metabolic changes in polarized macrophages by specifically targeting key glycolytic enzymes. However, extreme caution is required given the strong potential for off target effects. This is of particular importance in OA given that chondrocytes, in particular, exist in a hypoxic environment and rely on HIF1 α and glycolysis to maintain homeostasis. Currently, there are no drugs available to target BCP crystal deposition in the OA joint and subsequent inflammatory responses, however, based on the above findings, we propose that targeting BCP- and DAMP-induced metabolic reprogramming represents a novel avenue that requires further consideration and exploration.

Author contributions

OM and AD contributed to conception and design of the study, analysis and interpretation of the data, drafting of the article. DK and GM contributed to the interpretation of data and provision of study materials.

Competing interest statement

The authors declare no conflicts of interest.

Funding source

This study was supported by a Trinity College Dublin Post-graduate Research Studentship.

Acknowledgements

We would like to thank Dr Eoin O'Brien and Eva Desmond for technical assistance.

Supplementary data

Supplementary data to this article can be found online at <https://doi.org/10.1016/j.joca.2019.10.010>.

References

- Loeser RF, Collins JA, Diekmann BO. Ageing and the pathogenesis of osteoarthritis. *Nat Rev Rheumatol* 2016;12:412–20.
- Mobasheri A. The future of osteoarthritis therapeutics: targeted pharmacological therapy. *Curr Rheumatol Rep* 2013;15:364.
- O'Neill LAJ, Kishton RJ, Rathmell J. A guide to immunometabolism for immunologists. *Nat Rev Immunol* 2016;16:553–65.
- Pearce EL, Pearce EJ. Metabolic pathways in immune cell activation and quiescence. *Immunity* 2013;38:633–43.
- Pearce EL, Poffenberger MC, Chang C-H, Jones RG. Fueling immunity: insights into metabolism and lymphocyte function. *Science* 2013;342. 1242454.
- Loftus RM, Finlay DK. Immunometabolism: cellular metabolism turns immune regulator. *J Biol Chem* 2016;291:1–10.
- San-Millán I, Brooks GA. Reexamining cancer metabolism: lactate production for carcinogenesis could be the purpose and explanation of the Warburg Effect. *Carcinogenesis* 2017;38:119–33.
- Pålsson-McDermott EM, O'Neill LAJ. The Warburg effect then and now: from cancer to inflammatory diseases. *Bioessays* 2013;35:965–73.
- Dang EV, Barbi J, Yang H-Y, Jinasena D, Yu H, Zheng Y, et al. Control of T(H)17/T(reg) balance by hypoxia-inducible factor 1. *Cell* 2011;146:772–84.
- Russell DG, Huang L, VanderVen BC. Immunometabolism at the interface between macrophages and pathogens. *Nat Rev Immunol* 2019;19:291–304.
- Diskin C, Pålsson-McDermott EM. Metabolic modulation in macrophage effector function. *Front Immunol* 2018;9:270.
- Osborn O, Olefsky JM. The cellular and signaling networks linking the immune system and metabolism in disease. *Nat Med* 2012;18:363–74.
- Yin Y, Choi S-C, Xu Z, Perry DJ, Seay H, Croker BP, et al. Normalization of CD4+ T cell metabolism reverses lupus. *Sci Transl Med* 2015;7. 274ra18 LP-274ra18.
- Lee C-F, Lo Y-C, Cheng C-H, Furtmüller GJ, Oh B, Andrade-Oliveira V, et al. Preventing allograft rejection by targeting immune metabolism. *Cell Rep* 2017;13:760–70.
- Bettencourt IA, Powell JD. Targeting metabolism as a novel therapeutic approach to autoimmunity, inflammation, and transplantation. *J Immunol* 2017;198:999–1005.
- Biniecka M, Canavan M, McGarry T, Gao W, McCormick J, Cregan S, et al. Dysregulated bioenergetics: a key regulator of joint inflammation. *Ann Rheum Dis* 2016;75:2192–200.
- McGarry T, Biniecka M, Gao W, Cluxton D, Canavan M, Wade S, et al. Resolution of TLR2-induced inflammation through manipulation of metabolic pathways in Rheumatoid Arthritis. *Sci Rep* 2017;7:43165.

18. June RK, Liu-Bryan R, Long F, Griffin TM. Emerging role of metabolic signaling in synovial joint remodeling and osteoarthritis. *J Orthop Res* 2016;34:2048–58.
19. Liu-Bryan R. Inflammation and intracellular metabolism: new targets in OA. *Osteoarthr Cartil* 2015;23:1835–42.
20. Kluzek S, Newton JL, Arden NK. Is osteoarthritis a metabolic disorder? *Br Med Bull* 2015;115:111–21.
21. Mobasheri A, Rayman MP, Gualillo O, Sellam J, van der Kraan P, Fearon U. The role of metabolism in the pathogenesis of osteoarthritis. *Nat Rev Rheumatol* 2017;13:302–11.
22. Grishko VI, Ho R, Wilson GL, Pearsall AW. Diminished mitochondrial DNA integrity and repair capacity in OA chondrocytes. *Osteoarthr Cartil* 2009;17:107–13.
23. Gobelet C, Gerster JC. Synovial fluid lactate levels in septic and non-septic arthritides. *Ann Rheum Dis* 1984;43:742–5.
24. Bulysheva AA, Sori N, Francis MP. Direct crystal formation from micronized bone and lactic acid: the writing on the wall for calcium-containing crystal pathogenesis in osteoarthritis? *PLoS One* 2018;13. e0202373–e0202373.
25. McCarthy GM, Dunne A. Calcium crystal deposition diseases — beyond gout. *Nat Rev Rheumatol* 2018;14:592–602.
26. Stack J, McCarthy G. Basic calcium phosphate crystals and osteoarthritis pathogenesis: novel pathways and potential targets. *Curr Opin Rheumatol* 2016;28:122–6.
27. Nadra I, Mason JC, Philippidis P, Florey O, Smythe CDW, McCarthy GM, et al. Proinflammatory activation of macrophages by basic calcium phosphate crystals via protein kinase C and MAP kinase pathways. *Circ Res* 2005;96:1248–56.
28. Nasi S, So A, Combes C, Daudon M, Busso N. Interleukin-6 and chondrocyte mineralisation act in tandem to promote experimental osteoarthritis. *Ann Rheum Dis* 2016;75:1372–9.
29. Corr EM, Cunningham CC, Helbert L, McCarthy GM, Dunne A. Osteoarthritis-associated basic calcium phosphate crystals activate membrane proximal kinases in human innate immune cells. *Arthritis Res Ther* 2017;19.
30. Cunningham CC, Mills E, Mielke LA, O'Farrell LK, Lavelle E, Mori A, et al. Osteoarthritis-associated basic calcium phosphate crystals induce pro-inflammatory cytokines and damage-associated molecules via activation of Syk and PI3 kinase. *Clin Immunol* 2012;144.
31. Cunningham CC, Corr EM, McCarthy GM, Dunne A. Intra-articular basic calcium phosphate and monosodium urate crystals inhibit anti-osteoclastogenic cytokine signalling. *Osteoarthr Cartil* 2016;24.
32. Pazar B, Ea H-K, Narayan S, Kolly L, Bagnoud N, Chobaz V, et al. Basic calcium phosphate crystals induce monocyte/macrophage IL-1 β secretion through the NLRP3 inflammasome in vitro. *J Immunol* 2011;186:2495–502.
33. Corr EM, Cunningham CC, Helbert L, McCarthy GM, Dunne A. Osteoarthritis-associated basic calcium phosphate crystals activate membrane proximal kinases in human innate immune cells. *Arthritis Res Ther* 2017;19:23.
34. Nasi S, Ea H-K, Lioté F, So A, Busso N. Sodium thiosulfate prevents chondrocyte mineralization and reduces the severity of murine osteoarthritis. *PLoS One* 2016;11. e0158196.
35. Schulz D, Severin Y, Zanotelli VRT, Bodenmiller B. In-depth characterization of monocyte-derived macrophages using a mass cytometry-based phagocytosis assay. *Sci Rep* 2019;9: 1925.
36. Pergola C, Schubert K, Pace S, Zierysen J, Nikels F, Scherer O, et al. Modulation of actin dynamics as potential macrophage subtype-targeting anti-tumour strategy. *Sci Rep* 2017;7:1–12.
37. Zreiqat H, Belluoccio D, Smith MM, Wilson R, Rowley LA, Jones K, et al. S100A8 and S100A9 in experimental osteoarthritis. *Arthritis Res Ther* 2010;12. R16.
38. Van Lent PLEM, Blom AB, Schelbergen RFP, Slötjes A, Lafeber FPJG, Lems WF, et al. Active involvement of alarmins S100A8 and S100A9 in the regulation of synovial activation and joint destruction during mouse and human osteoarthritis. *Arthritis Rheum* 2012;64:1466–76.
39. Schelbergen RF, Blom AB, van den BMHJ, Annet S, Shahla A, Wim SB, et al. Alarmins S100A8 and S100A9 elicit a catabolic effect in human osteoarthritic chondrocytes that is dependent on Toll-like receptor 4. *Arthritis Rheum* 2011;64:1477–87.
40. Dominguez-Gutierrez PR, Kusmartsev S, Canales BK, Khan SR. Calcium oxalate differentiates human monocytes into inflammatory M1 macrophages. *Front Immunol* 2018;9:1863.
41. Kelly B, O'Neill LAJ. Metabolic reprogramming in macrophages and dendritic cells in innate immunity. *Cell Res* 2015;25: 771–84.
42. Everts B, Amiel E, Huang SCC, Smith AM, Chang CH, Lam WY, et al. TLR-driven early glycolytic reprogramming via the kinases TBK1-*IKK ϵ* supports the anabolic demands of dendritic cell activation. *Nat Immunol* 2014;15:323–32.
43. Thomas AC, Mattila JT. "Of mice and men": arginine metabolism in macrophages. *Front Immunol* 2014;5:1–7.
44. Everts B, Amiel E, Van Der Windt GJW, Freitas TC, Chott R, Yarasheski KE, et al. Commitment to glycolysis sustains survival of NO-producing inflammatory dendritic cells. *Blood* 2012;120:1422–31.
45. Malinarich F, Duan K, Hamid RA, Bijin A, Lin WX, Poidinger M, et al. High mitochondrial respiration and glycolytic capacity represent a metabolic phenotype of human tolerogenic dendritic cells. *J Immunol* 2015;194:5174–86.
46. McCarthy GM, Westfall PR, Masuda I, Christopherson PA, Cheung HS, Mitchell PG. Basic calcium phosphate crystals activate human osteoarthritic synovial fibroblasts and induce matrix metalloproteinase-13 (collagenase-3) in adult porcine articular chondrocytes. *Ann Rheum Dis* 2001;60:399–406.
47. Bai G, Howell DS, Howard GA, Roos BA, Cheung HS. Basic calcium phosphate crystals up-regulate metalloproteinases but down-regulate tissue inhibitor of metalloproteinase-1 and -2 in human fibroblasts. *Osteoarthr Cartil* 2001;9:416–22.
48. Morgan MP, Whelan LC, Sallis JD, McCarthy CJ, Fitzgerald DJ, McCarthy GM. Basic calcium phosphate crystal-induced prostaglandin E2 production in human fibroblasts: role of cyclooxygenase 1, cyclooxygenase 2, and interleukin-1 β . *Arthritis Rheum* 2004;50:1642–9.
49. Cunningham CC, Mills E, Mielke LA, O'Farrell LK, Lavelle E, Mori A, et al. Osteoarthritis-associated basic calcium phosphate crystals induce pro-inflammatory cytokines and damage-associated molecules via activation of Syk and PI3 kinase. *Clin Immunol* 2012;144:228–36.
50. Wang S, Song R, Wang Z, Jing Z, Wang S, Ma J. S100A8/A9 in inflammation. *Front Immunol* 2018;9:1298.
51. Johnson K, Jung A, Murphy A, Andreyev A, Dykens J, Terkeltaub R. Mitochondrial oxidative phosphorylation is a downstream regulator of nitric oxide effects on chondrocyte matrix synthesis and mineralization. *Arthritis Rheum* 2000;43:1560–70.
52. Wang Y, Zhao X, Lotz M, Terkeltaub R, Liu-Bryan R. Mitochondrial biogenesis is impaired in osteoarthritis chondrocytes but reversible via peroxisome proliferator-activated receptor γ coactivator 1 α . *Arthritis Rheum* 2015;67:2141–53.

53. Maneiro E, Martín MA, de Andres MC, López-Armada MJ, Fernández-Sueiro JL, del Hoyo P, *et al.* Mitochondrial respiratory activity is altered in osteoarthritic human articular chondrocytes. *Arthritis Rheum* 2003;48:700–8.
54. Blanco FJ, López-Armada MJ, Maneiro E. Mitochondrial dysfunction in osteoarthritis. *Mitochondrion* 2004;4:715–28.
55. Muz B, Larsen H, Madden L, Kiriakidis S, Paleolog EM. Prolyl hydroxylase domain enzyme 2 is the major player in regulating hypoxic responses in rheumatoid arthritis. *Arthritis Rheum* 2012;64:2856–67.
56. Tsai C-H, Chiang Y-C, Chen H-T, Huang P-H, Hsu H-C, Tang C-H. High glucose induces vascular endothelial growth factor production in human synovial fibroblasts through reactive oxygen species generation. *Biochim Biophys Acta - Gen Subj* 2013;1830:2649–58.